Inorganic Chemistry

including bioinorganic chemistry

March 3, 2014
Volume 53, Number 5
pubs.acs.org/IC

Modular N-Anchored Carbene and Phenolate Complexes

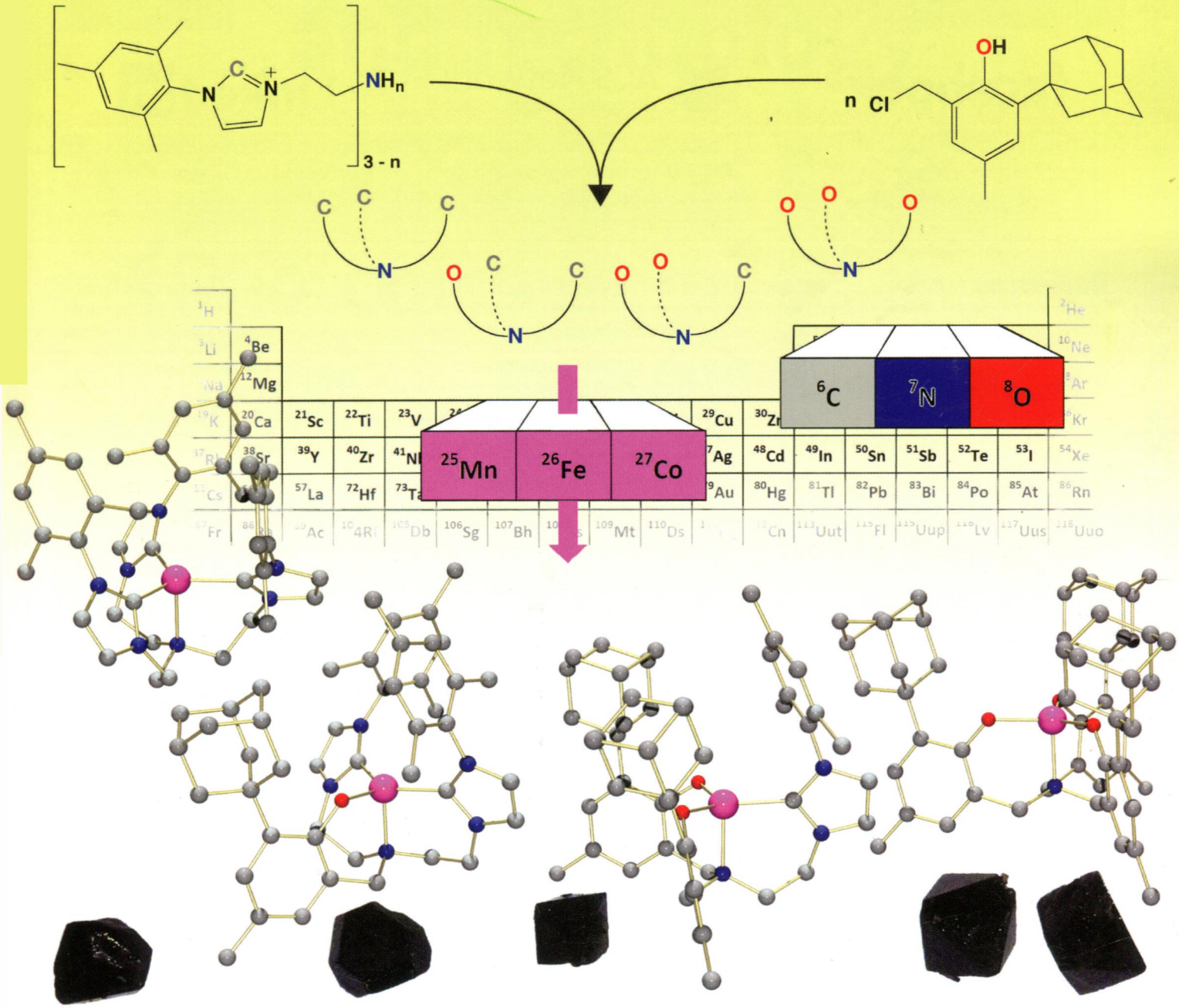

ACS Publications
MOST TRUSTED. MOST CITED. MOST READ.

www.acs.org

Inorganic Chemistry

MARCH 3, 2014
VOLUME 53 ISSUE 5

INOCAJ 53(5) 2343–2750 (2014)
ISSN 0020-1669
Registered in the U.S. Patent and Trademark Office

ON THE COVER: A series of N-anchored mixed carbene/phenolate ligands ranging from tris(carbene) to tris(phenolate) variants were synthesized and coordinated to manganese, iron, and cobalt ions. The structural, magnetic, and electronic properties of the resulting divalent complexes were investigated. See M. Käß, J. Hohenberger, M. Adelhardt, E. M. Zolnhofer, S. Mossin, F. W. Heinemann, J. Sutter, and K. Meyer, p 2460.

Communications

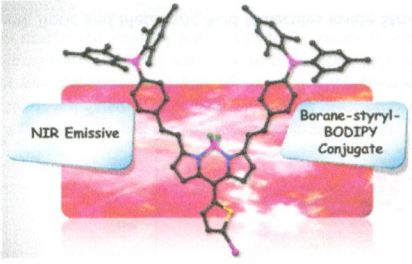

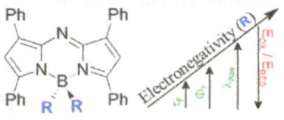

2349 S dx.doi.org/10.1021/ic402755q

Insight into the Gas-Phase Structure of a Copper(II) L-Histidine Complex, the Agent Used To Treat Menkes Disease
Blake E. Ziegler, Richard A. Marta, Michael B. Burt, and Terry B. McMahon*

The accompanying graphic is one of two lowest-energy structures found of the $[Cu(His)_2H]^+$ complex, which is supported by infrared multiple photon dissociation (IRMPD) data. Other structures have been investigated; however, the lowest-energy structures provide the best agreement with the IRMPD spectrum. These results demonstrate the power of the combined IRMPD and computational methods to probe gas-phase ionic structure.

2352 S dx.doi.org/10.1021/ic4027865

Homochiral Silver-Based Coordination Polymers Exhibiting Temperature-Dependent Photoluminescence Behavior
Xiaobing Xi, Yan Liu,* and Yong Cui*

Homochiral coordination polymers based on zigzag or helical polymers are assembled from a semiflexible fluorescent bipyridyl ligand and linear coordinated Ag^I ions; they exhibit unique temperature-dependent photoluminescence behavior, including multistep changes in energy and intensity upon cooling.

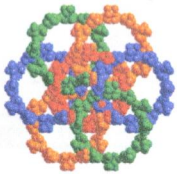

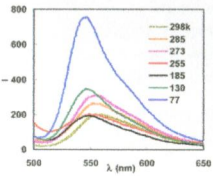

2355 S dx.doi.org/10.1021/ic4029832

Synthesis and Crystal Structure of the Rhenium(I) Tricarbonyl Complex of 5,10,15,20-Tetra-*p*-tolyl-21,23-dithiaporphyrin
Tejinder Kaur, Avijit Ghosh, Palanisamy Rajakannu, and Mangalampalli Ravikanth*

The unusual binding mode of rhenium(I) to two thiophene sulfur atoms and one of the pyrrole nitrogen atoms in the hexacoordinated complex of 5,10,15,20-tetra-*p*-tolyl-21,23-dithiaporphyrin.

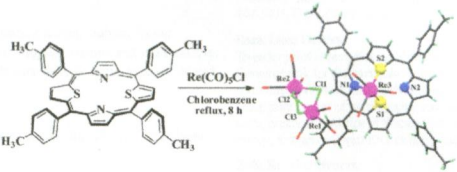

2358 dx.doi.org/10.1021/ic403070b

A New Cesium Pentaborate with New $B_{10}O_{19}$ Building Blocks

Anqing Jiao, Hongwei Yu, Hongping Wu,* Shilie Pan,* and Xingwen Zhang

The four polymorphs with the same chemical formula CsB_5O_8 all contain enclosing tunnels in the boron–oxygen anionic radical. All of the tunnels of different polymorphs are diverse in size and composition because of the different bond lengths and angles. The bond strain index and global instability index are calculated to compare their structural strains.

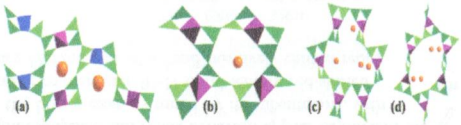

2361 dx.doi.org/10.1021/ic403081y

Redox Modulation of Magnetic Slow Relaxation in a 4f-Based Single-Molecule Magnet with a 4d Carbon-Rich Ligand

Lucie Norel,* Min Feng, Kevin Bernot,* Thierry Roisnel, Thierry Guizouarn, Karine Costuas, and Stéphane Rigaut*

A ruthenium carbon-rich-based ligand brings redox reversibility to a dysprosium-based single-molecule magnet. Long-distance perturbation of the 4f ion is achieved upon oxidation, resulting in an overall enhancement of the magnetic slow relaxation.

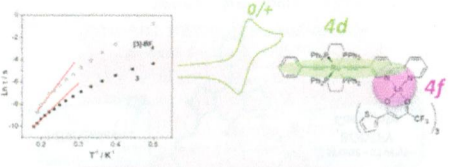

2364 dx.doi.org/10.1021/ic403175w

Open-Framework Gallium Borate with Boric and Metaboric Acid Molecules inside Structural Channels Showing Photocatalysis to Water Splitting

Wenliang Gao, Yan Jing, Jia Yang, Zhengyang Zhou, Dingfeng Yang, Junliang Sun, Jianhua Lin, Rihong Cong,* and Tao Yang*

We present a purely inorganic open-framework gallium borate, Ga-PKU-1, with intrinsic photocatalytic activity for water splitting that is superior to that of nanosized TiO_2. Its structural channels are occupied by neutral molecules, H_3BO_3 and $H_3B_3O_6$, making this the first example to experimentally show the structural template effect of boric acid in flux synthesis.

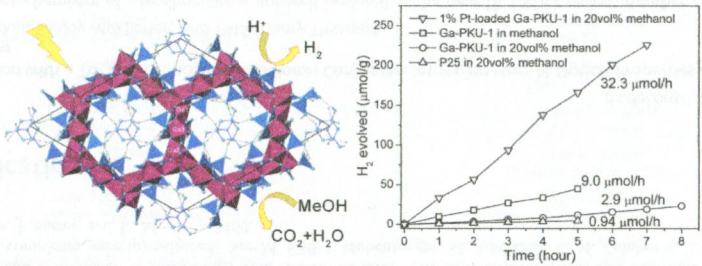

2367 S dx.doi.org/10.1021/ic5000638

Simple Mononuclear Cobalt(II) Complex: A Single-Molecule Magnet Showing Two Slow Relaxation Processes
Roman Boča,* Jozef Miklovič, and Ján Titiš

Complex $[Co(PPh_3)_2Br_2]$ possesses intermediate magnetic anisotropy, $D/hc = -13\ cm^{-1}$. It displays superparamagnetic behavior either in the absence of the magnetic field or in fields of $B_{dc} = 0.05$, 0.1, 0.15, and 0.2 T. At $B_{dc} = 0.1$ T, the barrier to spin reversal $U/k_B = 37$ K and the extrapolated relaxation time $\tau_0 = 9.4 \times 10^{-11}$ s confirm its classification as a single-molecule magnet. At $B_{dc} = 0.2$ T, two relaxation processes are evidenced.

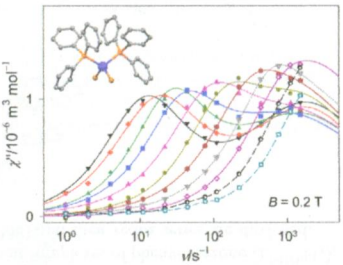

Articles

2370 S dx.doi.org/10.1021/ic4013137

Synthesis, Spectroscopy, and Hydrogen/Deuterium Exchange in High-Spin Iron(II) Hydride Complexes
Thomas R. Dugan, Eckhard Bill, K. Cory MacLeod, William W. Brennessel, and Patrick L. Holland*

The paramagnetic isotope effect on chemical shift (PIECS) in dimeric high-spin iron hydride complexes enabled detailed characterization of their structure, flexibility, and H/D exchange reactions.

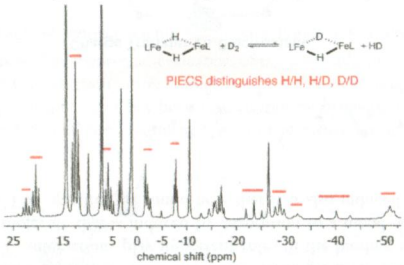

2381 S

dx.doi.org/10.1021/ic401395d

Highly Enhanced Bisignate Circular Dichroism of Ferrocene-Bridged Zn(II) Bisporphyrin *Tweezer* with Extended Chiral Substrates due to Well-Matched Host–Guest System

Sanfaori Brahma, Sk Asif Ikbal, Avinash Dhamija, and Sankar Prasad Rath*

Four new supramolecular chiral *tweezer*-diamine complexes consisting of an achiral Zn(II)bisporhyrin host (green line) and two small chiral diamines, (1*R*,2*R*)-DPEA and (1*S*,2*S*)-CHDA, and two large extended chiral diamines, (1*R*,2*R*)-DPEApy and (1*S*,2*S*)-CHDApy, are reported. Complexes with extended chiral substrates show remarkably high amplitude of bisignate CD signal (blue line), while smaller substrates show low value (red line) with opposite sign of CD couplet.

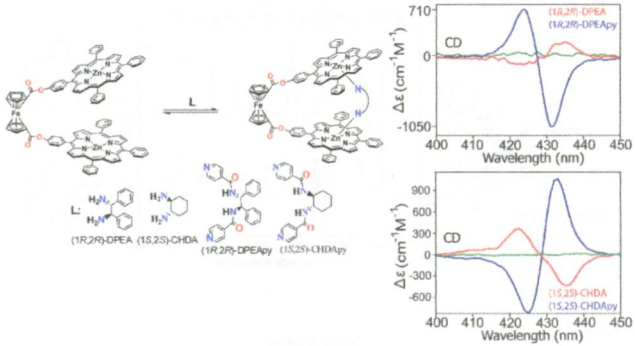

2396 S

dx.doi.org/10.1021/ic401731a

Chemistry and Biology of Two Novel Gold(I) Carbene Complexes as Prospective Anticancer Agents

Luigi Messori, Lorella Marchetti, Lara Massai, Federica Scaletti, Annalisa Guerri, Ida Landini, Stefania Nobili, Gabriele Perrone, Enrico Mini, Piero Leoni, Marco Pasquali, and Chiara Gabbiani*

Two novel gold carbene compounds manifested similarly potent cytotoxic actions in vitro against A2780 human ovarian carcinoma cells, and both were able to completely overcome resistance to cisplatin in the A2780R line. Relevant metalation effects were highlighted with the Atox-1 protein, suggesting that the investigated gold carbene complexes most probably act through selective metalation of a few proteins bearing specific gold binding motifs.

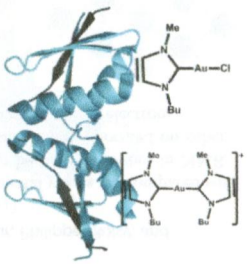

2404 dx.doi.org/10.1021/ic402048a

Ring-Closing Metathesis and Nanoparticle Formation Based on Diallyldithiocarbamate Complexes of Gold(I): Synthetic, Structural, and Computational Studies

Saira Naeem, Stefano A. Serapian, Anita Toscani, Andrew J. P. White, Graeme Hogarth, and James D. E. T. Wilton-Ely*

From molecules to materials: investigations of ring-closing metathesis of coordinated diallyldithiocarbamate gold(I) complexes have led to the discovery of a single component dithiocarbamate precursor for gold nanoparticles. Calculations indicate that the gold-dithiocarbamate interactions are substantially different from those established in theoretical and experimental studies on thiol-coated gold nanoparticles.

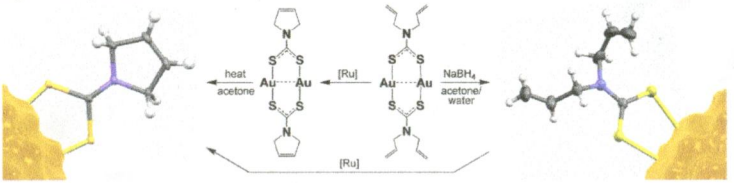

2417 dx.doi.org/10.1021/ic402172v

Interaction of Various Gas Molecules with Paddle-Wheel-Type Open Metal Sites of Porous Coordination Polymers: Theoretical Investigation

Yuh Hijikata and Shigeyoshi Sakaki*

The interaction of the Cu paddle-wheel-type open metal site with various gas molecules was theoretically investigated. The electrostatic and charge-transfer (CT) interactions play important roles in the binding of gas molecules. Although the vibrational frequency shift in a gas molecule that is induced by adsorption to a metal−organic framework (MOF) has been discussed in general based on the CT interaction, we found here that it is also induced by the electrostatic potential by the MOF.

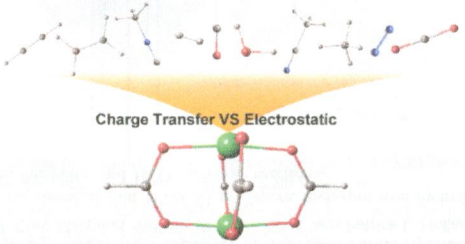

2427 dx.doi.org/10.1021/ic4022432

Ruthenium, Rhodium, Osmium, and Iridium Complexes of Osazones (Osazones = Bis-Arylhydrazones of Glyoxal): Radical versus Nonradical States

Sarat Chandra Patra, Thomas Weyhermüller, and Prasanta Ghosh*

Molecular and electronic structures of the ruthenium, rhodium, osmium, and iridium complexes of phenyl osazone ($L^{NHPh}H_2$), benzoyl osazone ($L^{NHCOPh}HR$; R = H, Me), and anilido osazone ($L^{NHCONHPh}HMe$) and their redox series are disclosed.

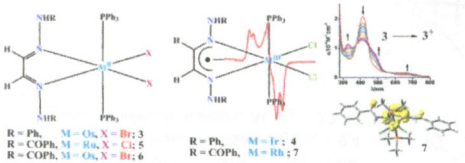

2441 dx.doi.org/10.1021/ic4023536

Supramolecular 2D/3D Isomerism in a Compound Containing Heterometallic $Cu^{II}_2Co^{II}$ Nodes and Dicyanamide Bridges

Saptarshi Biswas, Carlos J. Gómez-García, Juan M. Clemente-Juan, Samia Benmansour, and Ashutosh Ghosh*

Among three heterometallic complexes that were synthesized by trinuclear $Cu^{II}_2Co^{II}$ nodes and dicyanamide spacers, two are very rare supramolecular 2D/3D isomers and can be identified by different colors. The presence of moderate antiferromagnetic exchange interactions in the complexes are fitted with an anisotropic model including spin−orbit coupling in the central Co(II) ion.

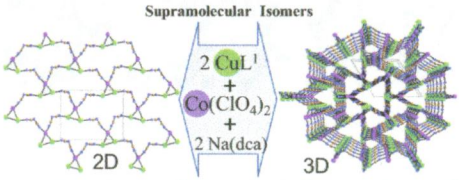

2450 dx.doi.org/10.1021/ic402371x

Paramagnetism of Aqueous Actinide Cations. Part I: Perchloric Acid Media

Thomas F. Wall,* Steve Jan, Matthieu Autillo, Kenneth L. Nash, Laetitia Guerin, Claire Le Naour, Philippe Moisy, and Claude Berthon*

Magnetic susceptibilities of soluble actinide ions were revisited by NMR spectroscopy. Experimental values are compared with previously published values. An estimated order of magnitude of the paramagnetic effects can be used as probes in NMR spectroscopy. Lanthanide(III) ions are discussed in the context of 4f and 5f electrons. Measurements performed on other actinide oxidation states (IV, V, and VI) emphasize the importance of water ligand field effects on the 5f electrons.

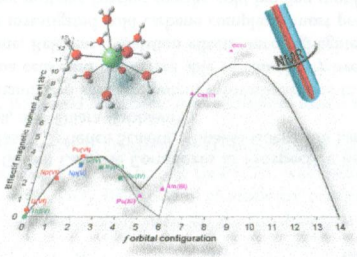

2460 (S) dx.doi.org/10.1021/ic4024053

Synthesis and Characterization of Divalent Manganese, Iron, and Cobalt Complexes in Tripodal Phenolate/N-Heterocyclic Carbene Ligand Environments

Martina Käß, Johannes Hohenberger, Mario Adelhardt, Eva M. Zolnhofer, Susanne Mossin, Frank W. Heinemann, Jörg Sutter, and Karsten Meyer*

Two novel mixed NHC/phenolate ligands, $(BIMPN^{Mes,Ad,Me})^-$ and $(MIMPN^{Mes,Ad,Me})^{2-}$, were synthesized to complete a tripodal N-anchored ligand series, ranging from tris(carbene) to tris(phenolate). The ligand series offers convenient tunability of the electronic and steric environment around the metal center. The new chelates' coordination chemistry to Mn, Fe, and Co was explored, and a range of complexes of divalent Mn, Fe, and Co were thoroughly characterized. Trends in structural, ^{57}Fe Mössbauer, and magnetization parameters are discussed.

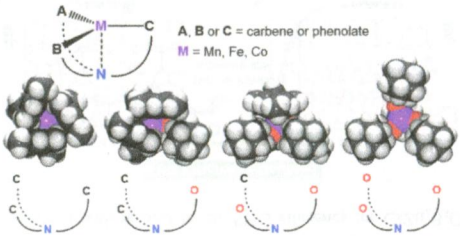

2471 (S) dx.doi.org/10.1021/ic402414f

Synthesis and Theoretical Investigations of the Solid Solution $CeRu_{1-x}Ni_xAl$ (x = 0.1−0.95) Showing Cerium Valence Fluctuations

Oliver Niehaus, Ute Ch. Rodewald, Paula M. Abdala, Rachid St. Touzani, Boniface P. T. Fokwa, and Oliver Janka*

The synthesis and characterization as well as theoretical evaluation of the solid solution $CeRu_{1-x}Ni_xAl$ (x = 0.1−0.85), which exhibits valence fluctuations along with a reduction of the average cerium valence based upon the nickel content in the system, have been investigated. The mixed-valent character has been investigated by magnetic susceptibility measurements and XANES. Theoretical calculations have shown that a significant amount of ruthenium is necessary in order to stabilize the orthorhombic modification.

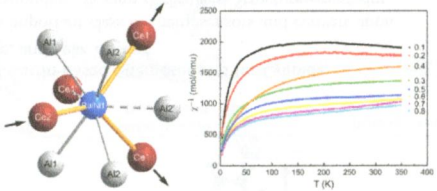

2481 S dx.doi.org/10.1021/ic402474t

Infrared Vibrational Spectroscopy of $[Ru(bpy)_2(bpm)]^{2+}$ and $[Ru(bpy)_3]^{2+}$ in the Excited Triplet State

Tatsuhiko Mukuta, Naoto Fukazawa, Kei Murata, Akiko Inagaki, Munetaka Akita, Sei'ichi Tanaka, Shin-ya Koshihara, and Ken Onda*

We have comprehensively investigated the infrared vibrational spectra of $[Ru(bpy)_2(bpm)]^{2+}$ and $[Ru(bpy)_3]^{2+}$ using time-resolved infrared spectroscopy. We assigned almost all of the observed bands to the calculated normal modes in the fingerprint region. Moreover, the characteristic bands assigned to the neutral ligands (bpy^0) are commonly observed in both complexes, although the excited electron is localized on a single ligand (bpy^- or bpm^-).

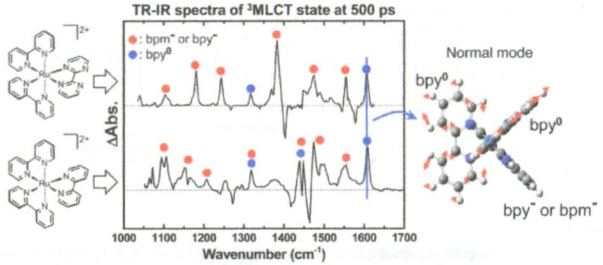

2491 S dx.doi.org/10.1021/ic402514n

In Situ Energy-Dispersive X-ray Diffraction for the Synthesis Optimization and Scale-up of the Porous Zirconium Terephthalate UiO-66

Florence Ragon, Patricia Horcajada,* Hubert Chevreau, Young Kyu Hwang, U-Hwang Lee, Stuart R. Miller, Thomas Devic, Jong-San Chang, and Christian Serre*

In situ energy-dispersive X-ray diffraction studies for the understanding and scale-up of the porous zirconium terephthalate UiO-66(Zr). The crystallization of the porous metal–organic framework UiO-66(Z) was studied by in situ energy-dispersive X-ray diffraction experiments to approach its formation and investigate the influence of different synthetic conditions. These experiments allow optimizing and up-scaling the synthesis of this phase at the 0.5 kg scale.

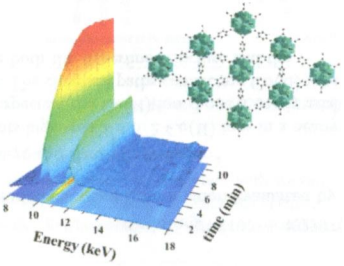

2501 S dx.doi.org/10.1021/ic4025525

Two New Barium Borate Fluorides $ABa_{12}(BO_3)_7F_4$ (A = Li and Na)

Jing Zhao and R. K. Li*

$ABa_{12}(BO_3)_7F_4$ (A = Li and Na) is crystallized into the tetragonal system, with space group *I*4/*mcm*. In the structure there are tunnels directed along the *c* axis, which are occupied by alkaline fluoride salt Li/NaF_4 and BO_3 groups. The Li cations in the tunnel have high conductivity at elevated temperatures.

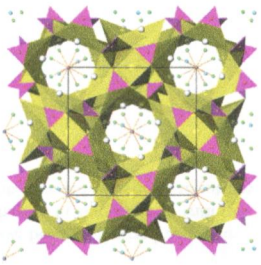

2506 S dx.doi.org/10.1021/ic4026359

Toward Equatorial Planarity about Uranyl: Synthesis and Structure of Tridentate Nitrogen-Donor $\{UO_2\}^{2+}$ Complexes

Roy Copping,* Byoungseon Jeon, C. Das Pemmaraju, Shuao Wang, Simon J. Teat, Markus Janousch, Tolek Tyliszczak, Andrew Canning,* Niels Grønbech-Jensen, David Prendergast,* and David K. Shuh*

The reaction of $UO_2Cl_2{\cdot}3THF$ with the tridentate nitrogen donor ligand 2,6-bis(2-benzimidazolyl)pyridine (H_2BBP) in pyridine leads to the formation of three different complexes, $[(UO_2)(H_2BBP)Cl_2]$, $[(UO)_2(HBBP)(Py)Cl]$, and $[(UO_2)(BBP)(Py)_2]$, after successive deprotonation of H_2BBP with a strong base. Crystallographic determination of these complexes reveals that increased charge through ligand deprotonation and displacement of chloride leads to equatorial planarity about uranyl as well as a more compact overall coordination geometry.

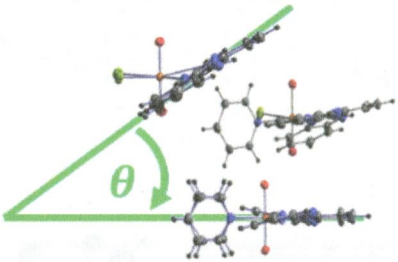

2516 S dx.doi.org/10.1021/ic4026427

Controlling Binding Dynamics of Corrin-Based Chemosensors for Cyanide

Balz Aebli, Christine Männel-Croisé, and Felix Zelder*

Aquacyanocorrinoids represent an important class of chemosensors and convert upon cyanide coordination to the corresponding dicyano derivatives. Structure−reactivity relationships were investigated by synthesizing and studying three diastereomerically pure aquacyanocorrinoids with key structural differences. Stopped-flow measurements were made, and second order rate constants and activation parameters were determined. In particular, it is demonstrated that the binding kinetics depend on (i) the configuration at the central metal center and on (ii) remote structural modifications of the macrocycle.

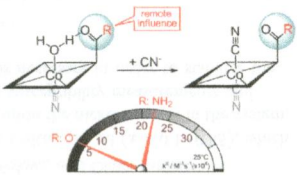

2521 S dx.doi.org/10.1021/ic402667m

A New UV Nonlinear Optical Material $CsZn_2B_3O_7$: ZnO_4 Tetrahedra Double the Efficiency of Second-Harmonic Generation

Sangen Zhao, Jia Zhang, Shu-quan Zhang, Zhihua Sun, Zheshuai Lin,* Yicheng Wu, Maochun Hong, and Junhua Luo*

ZnO_4 tetrahedra lead to a 2-fold contrast with respect to the SHG efficiency for $CsZn_2B_3O_7$ in comparison with the structurally analogous γ-$KBe_2B_3O_7$.

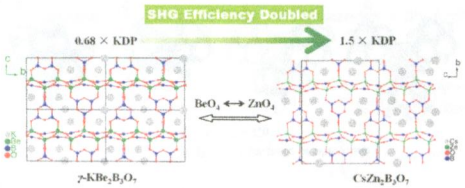

2528 dx.doi.org/10.1021/ic402672m

Structure, Magnetic Behavior, and Anisotropy of Homoleptic Trinuclear Lanthanoid 8-Quinolinolate Complexes

Nicholas F. Chilton, Glen B. Deacon, Olga Gazukin, Peter C. Junk,* Berthold Kersting, Stuart K. Langley, Boujemaa Moubaraki, Keith S. Murray, Frederik Schleife, Mahasish Shome, David R. Turner, and Julia A. Walker

Three complexes of the form $[Ln^{III}_3(OQ)_9]$ (Ln = Gd, Tb, Dy; OQ = 8-quinolinolate) have been synthesized and their magnetic properties studied. The dysprosium complex displays single-molecule-magnet behavior, in zero dc field, with two distinct relaxation modes of differing time scales within the same molecule. Analysis of the data revealed substantial anisotropy barriers of U_{eff} = 92 and 48 K for the two processes.

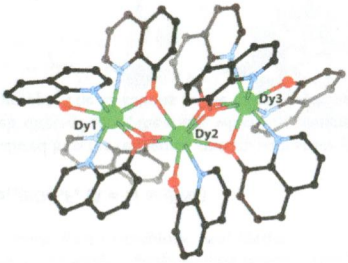

2535 dx.doi.org/10.1021/ic402797t

Magnetic Properties of Weakly Exchange-Coupled High Spin Co(II) Ions in Pseudooctahedral Coordination Evaluated by Single Crystal X-Band EPR Spectroscopy and Magnetic Measurements

Nicolás I. Neuman, Elín Winkler, Octavio Peña, Mario C. G. Passeggi, Alberto C. Rizzi, and Carlos D. Brondino*

The coordination polymer *catena*-(*trans*-(μ_2-fumarato)tetraaquacobalt(II)) presents high spin $S = 3/2$ Co(II) ions in a nearly octahedral environment linked by hydrogen bonds and fumarate molecules. As expected, the Co(II) ion shows a nearly axial g′-tensor ($g'_3 < g'_1 \approx g'_2$), but not following the pseudosymmetry of the cobalt site. The chemical paths connecting Co(II) ions transmit very weak exchange interactions (J_{AA} and J_{AB}) strong enough to merge both the hyperfine structure and the inequivalent Co(II) ion resonances.

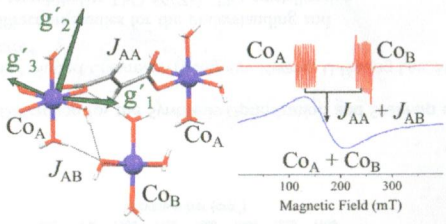

2545 S dx.doi.org/10.1021/ic402843y

Trinuclear Manganese Complexes of Unsymmetrical Polypodal Diamino N_3O_3 Ligands with an Unusual $[Mn_3(\mu\text{-}OR)_4]^{5+}$ Triangular Core: Synthesis, Characterization, and Catalase Activity

Gabriela N. Ledesma, Elodie Anxolabéhère-Mallart, Eric Rivière, Sonia Mallet-Ladeira, Christelle Hureau,* and Sandra R. Signorella*

Unsymmetrical N_3O_3 ligands derived from 1,3-diaminopropan-2-ol (H_3L) afford a new type of trinuclear Mn^{III}_3 complexes with the bis(μ-alkoxo)(μ-phenoxo)(μ-hydroxo)triMn^{III} core and general formula $[Mn_3L_2(\mu\text{-}OH)(OAc)]ClO_4$. These compounds possess one labile site for substrate binding on the Mn ion at the apex of a near isosceles triangle and catalyze H_2O_2 decomposition employing the $[Mn_3L_2(\mu\text{-}O)]^+$ active form.

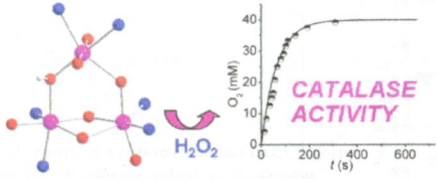

2554 S dx.doi.org/10.1021/ic402855r

Cooperative Anion Recognition in Copper(II) and Zinc(II) Complexes with a Ditopic Tripodal Ligand Containing a Urea Group

Israel Carreira-Barral, Teresa Rodríguez-Blas, Carlos Platas-Iglesias, Andrés de Blas, and David Esteban-Gómez*

The Cu^{II} and Zn^{II} complexes of a urea ditopic receptor allow recognition of SO_4^{2-} and Cl^- anions through cooperative binding involving simultaneous coordination to the metal ion and different hydrogen-bonding interactions. The unprecedented N-coordination of the urea unit to the metal ion increases the acidity of one of its N–H groups, which is deprotonated upon addition of basic anions such as $MeCO_2^-$ or F^-.

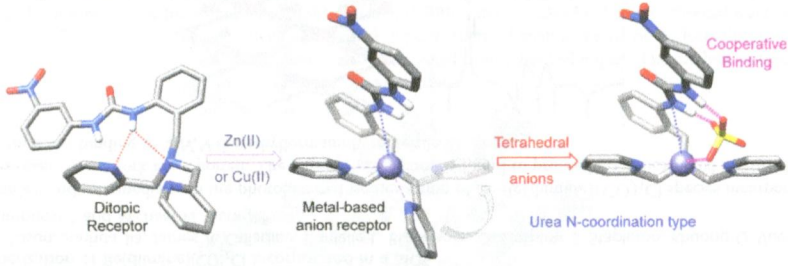

2569 dx.doi.org/10.1021/ic4028628

Linker Conformation Effects on the Band Gap in Metal–Organic Frameworks

Espen Flage-Larsen* and Knut Thorshaug

In the metal–organic framework UiO-68-R, the band gaps and torsional angle of the middle aromatic ring depend on the choice of R. Band-gap modulation by the judicious choice of R is shown to be possible.

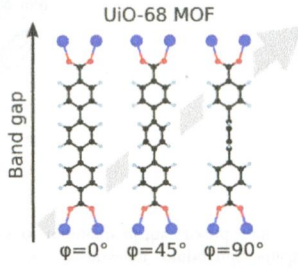

2573 dx.doi.org/10.1021/ic402879g

Photoinduced Dimerization Reaction Coupled with Oxygenation of a Platinum(II)–Hydrazone Complex

Atsushi Kobayashi,* Daisuke Yamamoto, Hiroyuki Horiki, Kana Sawaguchi, Takeshi Matsumoto, Kiyohiko Nakajima, Ho-Chol Chang, and Masako Kato*

Evaluation of the photochemical reactions of metal(II)–hydrazone complexes demonstrated the interesting photodimerization reaction of the Pt(II)–hydrazone complex coupled with oxygenation of the hydrazone moiety. The Ni(II) complex with the same hydrazone ligand showed no change, and the hydrazone ligand was simply photo-oxidized at the phosphine moiety.

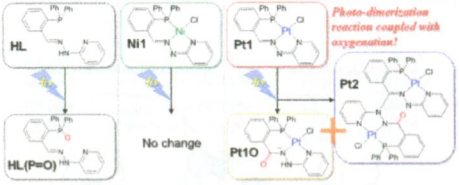

2582 dx.doi.org/10.1021/ic4028964

Anisotropic Iron Motion in Nitrosyl Iron Porphyrinates: Natural and Synthetic Hemes

Jeffrey W. Pavlik, Qian Peng, Nathan J. Silvernail, E. Ercan Alp, Michael Y. Hu, Jiyong Zhao, J. Timothy Sage,* and W. Robert Scheidt*

The oriented single-crystal iron vibrations in the five-coordinate low-spin [Fe(Porph)(NO)] have been examined by nuclear resonance vibration spectrospcy (NRVS). The NO orientation has a strong effect on the in-plane iron motion in both synthetic and natural heme derivatives.

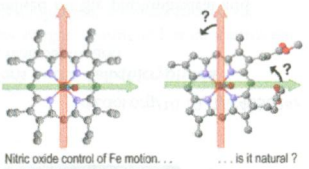

2591 dx.doi.org/10.1021/ic402944r

Light-Atom Influences on the Electronic Structures of Iron–Sulfur Clusters

Christopher J. Pollock, Lay Ling Tan, Wei Zhang, Kyle M. Lancaster, Sonny C. Lee,* and Serena DeBeer*

Sulfur and chlorine K-edge X-ray absorption spectroscopy is applied to dimeric and tetrameric Fe–S clusters with varying numbers of imido ligands to gain insight into the influence of light atoms on Fe–S clusters. These experimental results, combined with theory, are utilized to obtain insight into how the central C^{4-} in the FeMo cofactor of nitrogenase could modulate the electronic structure of the cluster.

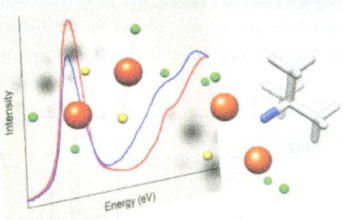

2598 Ⓢ dx.doi.org/10.1021/ic402950j

Structural and Electronic Dependence of the Single-Molecule-Magnet Behavior of Dysprosium(III) Complexes

Victoria E. Campbell,* Hélène Bolvin, Eric Rivière, Regis Guillot, Wolfgang Wernsdorfer, and Talal Mallah*

A subtle modification in a ligand resulted in the synthesis of two isostructural mononuclear dysprosium compounds, which have different magnetic behaviors. First-principles calculations indicated that the magnetic moments of the ground-state Kramers doublet are different in the two complexes.

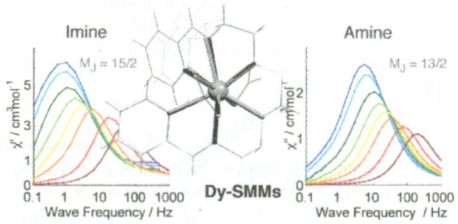

2606 dx.doi.org/10.1021/ic402955e

Photochemistry in a 3D Metal–Organic Framework (MOF): Monitoring Intermediates and Reactivity of the *fac*-to-*mer* Photoisomerization of Re(diimine)$(CO)_3$Cl Incorporated in a MOF

Timothy L. Easun, Junhua Jia, James A. Calladine, Danielle L. Blackmore, Christopher S. Stapleton, Khuong Q. Vuong, Neil R. Champness,* and Michael W. George*

The mechanism and intermediates in the photoinitiated isomerization of *fac*-Re(diimine)$(CO)_3$Cl species incorporated into a 3D metal–organic framework are reported. The *fac*–*mer* conversion is found to proceed via a dicarbonyl intermediate, which undergoes transient binding to a *N*,*N*-dimethylformamide molecule.

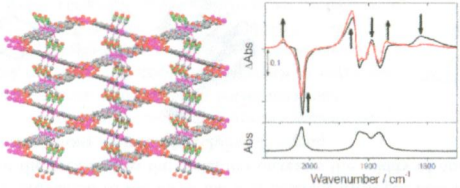

2613 Ⓢ dx.doi.org/10.1021/ic402971a

Toward Higher Nuclearity: Tetranuclear Cobalt(II) Metallogrid Exhibiting Spin Crossover

Shu-Qi Wu, Yi-Tong Wang, Ai-Li Cui, and Hui-Zhong Kou*

A supramolecular strategy of designing grid-type cobalt(II) spin-crossover complex is adopted to obtain the highest nuclearity Co^{II} spin-crossover cluster. Both mononuclear and tetranuclear Co^{II} complexes display SCO behavior. Moreover, the spin transition in Co_4^{II} cluster is a two-step process rarely reported in literature.

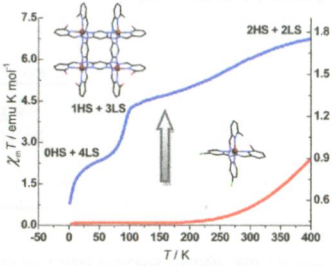

2619 S dx.doi.org/10.1021/ic402974k

A Supramolecular Double Sulfate Salt with a Lamellar Type: Crystal Structure and Thermal Behavior

Omar Kammoun, Thierry Bataille,* Anita Lucas, Vincent Dorcet, Isabelle Marlart, Walid Rekik, Houcine Naïli, and Tahar Mhiri

Double sulfates of transition metal and α-methylbenzylamine have been obtained as supramolecular double salts. Their crystal structure shows an unprecedented lamellar type with a significant interlayer distance of more than 16 Å. The compounds behave as organically intercalated-clay materials, when submitted to temperature increase, with important differences according to the metal.

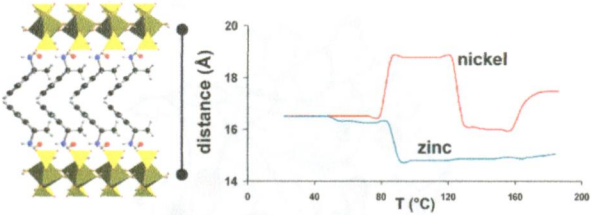

2628 dx.doi.org/10.1021/ic4030124

Rapid Microwave Preparation and ab Initio Studies of the Stability of the Complex Noble Metal Oxides La_2BaPdO_5 and La_2BaPtO_5

Lauren M. Misch, Jakoah Brgoch, Alexander Birkel, Thomas E. Mates, Galen D. Stucky, and Ram Seshadri*

Microwave-assisted methods allow stable complex oxides of Pd and Pt to be rapidly prepared; ab initio calculations of absolute energy levels suggest reasons for the enhanced stability of these oxides toward reduction.

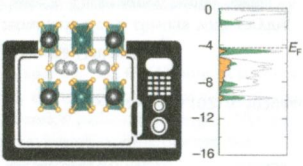

2635 S dx.doi.org/10.1021/ic403024z

Revisited Photophysics and Photochemistry of a Ru-TAP Complex Using Chloride Ions and a Calix[6]crypturea

Mateusz Rebarz, Lionel Marcélis, Mickaël Menand, Damien Cornut, Cécile Moucheron, Ivan Jabin, and Andrée Kirsch-De Mesmaeker*

The effects of the nonprotonated and protonated calix[6]crypturea **1**/**1**•H$^+$ were examined on the photophysical and photochemical behavior of the PF_6^- and Cl^- salts of $[Ru(TAP)_2phen]^{2+}$ in MeCN and BuCN.

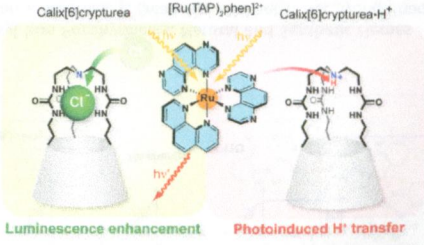

2645 dx.doi.org/10.1021/ic403030w

Structural, Electronic, and Optical Features of $CuAl(S_{1-x}Se_x)_2$ Solar Cell Materials

M. G. Brik,* M. Piasecki, and I. V. Kityk

The structural, electronic, and optical properties of solid solutions of the promising solar cell material $CuAl(S_{1-x}Se_x)_2$ over the whole range of Se concentration from $x = 0$ to $x = 1$ were calculated. The lattice parameters, band gap, and anisotropic refractive indices vary linearly with the Se concentration. The obtained linear dependences allow for reliable estimations of all these quantities for any value of x, which can be used in a straightforward way for the successful production of $CuAl(S_{1-x}Se_x)_2$ mixed compounds with desired optoelecronic parameters.

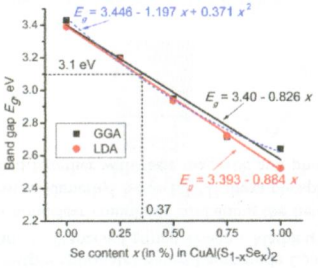

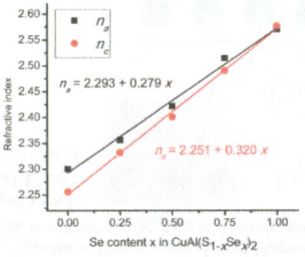

2652 dx.doi.org/10.1021/ic403033j

Synthesis, Structural Elucidation, and Catalytic Properties in Olefin Epoxidation of the Polymeric Hybrid Material $[Mo_3O_9(2\text{-}[3(5)\text{-Pyrazolyl}]pyridine)]_n$

Tatiana R. Amarante, Patrícia Neves, Ana C. Gomes, Mariela M. Nolasco, Paulo Ribeiro-Claro, Ana C. Coelho, Anabela A. Valente, Filipe A. Almeida Paz,* Stef Smeets, Lynne B. McCusker, Martyn Pillinger, and Isabel S. Gonçalves*

The molybdenum oxide/pyrazolylpyridine polymeric hybrid material $[Mo_3O_9(pzpy)]_n$ (**2**) (pzpy = 2-[3(5)-pyrazolyl]-pyridine) has been prepared by the reaction of $[MoO_2Cl_2(pzpy)]$ with water and also by the hydrothermal reaction of MoO_3, pzpy, and water. The structure of **2** was solved and refined through Rietveld analysis based on high-resolution synchrotron powder X-ray diffraction data in conjunction with information obtained from other techniques. The catalytic potential of **2** was investigated in the epoxidation of the model substrate *cis*-cyclooctene.

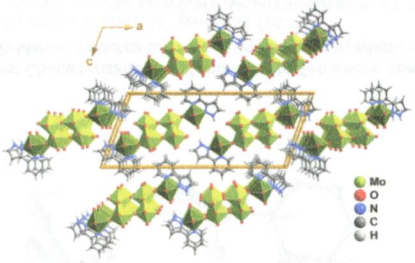

2666 S

dx.doi.org/10.1021/ic403057k

Triniobium, Wells–Dawson-Type Polyoxoanion, $[(n\text{-}C_4H_9)_4N]_9P_2W_{15}Nb_3O_{62}$: Improvements in the Synthesis, Its Reliability, the Purity of the Product, and the Detailed Synthetic Procedure

William W. Laxson, Saim Özkar, and Richard G. Finke*

An improved synthetic procedure is reported for reliably producing the highest available purity $[(n\text{-}C_4H_9)_4N]_9P_2W_{15}Nb_3O_{62}$ to date. The experimentally independently checked procedure is the result of additional extensive experimentation over ca. 2 years and above the six prior syntheses, including an *Inorganic Syntheses* procedure. Considerable emphasis is given to the problem of detailing a written experimental procedure that proved reproducible by an independent researcher working from only that written procedure.

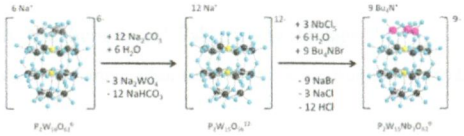

2677 S

dx.doi.org/10.1021/ic4030712

Direct Observation of Reversible Electronic Energy Transfer Involving an Iridium Center

Sergey A. Denisov, Yanouk Cudré, Peter Verwilst, Gediminas Jonusauskas, Marta Marín-Suárez, Jorge Fernando Fernández-Sánchez, Etienne Baranoff,* and Nathan D. McClenaghan*

A cyclometalated iridium complex with an appended pyrene unit is reported to have a remarkably long excited-state lifetime (225 μs) due to an efficient reversible electronic energy transfer between the two chromophores, as evidenced by time-resolved spectroscopies. As a result, the complex is among the best iridium complexes for oxygen sensing at low concentration.

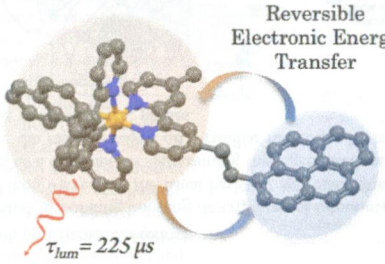

2683 S

dx.doi.org/10.1021/ic403077q

Tetracarboxylate Ligands as New Chelates Supporting Copper(II) Paddlewheel-Like Structures

Antoine Gomila, Sylvain Duval, Céline Besnard, Karl W. Krämer, Shi-Xia Liu, Silvio Decurtins, and Alan F. Williams*

Two new ligands carrying four carboxylate functions designed to bridge metal centers give rise to new polynuclear complexes with copper.

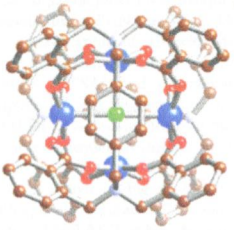

2692 S dx.doi.org/10.1021/ic403098p

Synthesis, Structural, Spectroscopic, and Magnetic Characterization of Two-Coordinate Cobalt(II) Aryloxides with Bent or Linear Coordination

Aimee M. Bryan, Gary J. Long,* Fernande Grandjean, and Philip P. Power*

The first two-coordinate cobalt(II) aryloxide complexes $Co(OAr^{Me_6})_2$ (**1**) and $Co(OAr^{iPr_4})_2$ (**2**) ($Ar^{Me_6} = C_6H_3$-2,6(C_6H_2-2,4,6-Me_3)$_2$; $Ar^{iPr_4} = C_6H_3$-2,6(C_6H_3-2,6-Pr^i_2)$_2$) were synthesized by amine elimination reactions of $HOAr^{Me_6}$ and $HOAr^{iPr_4}$ with $[Co\{N(SiMe_3)_2\}_2]_2$. Elimination to give **1** afforded a 95.0(8)% occupancy of the cobalt site, and **2** was shown to afford 84.6% and 93.5% occupancies depending on the reaction conditions. The analysis of the temperature dependence of $\chi_M T$ combines crystal field effects and spin−orbit coupling for the $S = 3/2$, $L = 2$ cobalt(II) ions.

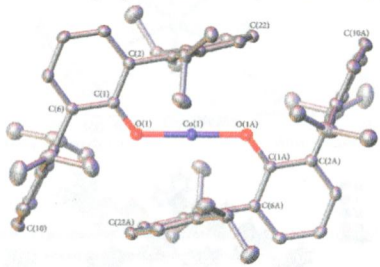

2699 S dx.doi.org/10.1021/ic4031014

Copper Diamidocarbene Complexes: Characterization of Monomeric to Tetrameric Species

Lee R. Collins, John P. Lowe, Mary F. Mahon, Rebecca C. Poulten, and Michael K. Whittlesey*

Treatment of CuCl with the diamidocarbene 6-MesDAC generated [(6-MesDAC)CuCl]$_2$, [(6-MesDAC)$_2$(CuCl)$_3$], and [(6-MesDAC)$_2$(CuCl)$_4$]. Efforts to convert the dimer to a Cu−O^{t}Bu complex led instead to a partially metathesized ate complex; attempts at crystallization afforded instead a 1:1 mixture of [(6-MesDAC)CuCl]$_2$ and [(6-MesDAC)CuCl].

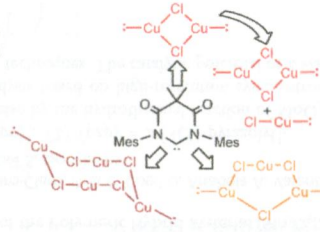

2708 S dx.doi.org/10.1021/ic403104y

Cyanomethylene-bis(phosphonate)-Based Lanthanide Complexes: Structural, Photophysical, and Magnetic Investigations

Catalin Maxim, Diana G. Branzea, Carmen Tiseanu, Mathieu Rouzières, Rodolphe Clérac, Marius Andruh, and Narcis Avarvari*

Ten lanthanide mononuclear complexes containing the heteroditopic ligand cyanomethylene-bis(5,5-dimethyl-2-oxo-1,3,2λ^5-dioxa-phosphorinane) **L** are structurally described together with their magnetic and photophysical properties.

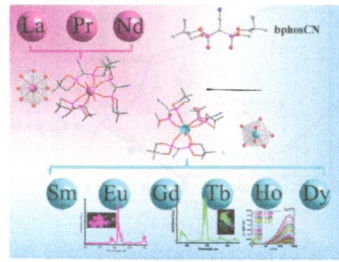

2718 S dx.doi.org/10.1021/ic4031359

Ruthenium-Nitrosyl Complexes with Glycine, L-Alanine, L-Valine, L-Proline, D-Proline, L-Serine, L-Threonine, and L-Tyrosine: Synthesis, X-ray Diffraction Structures, Spectroscopic and Electrochemical Properties, and Antiproliferative Activity

Anna Rathgeb, Andreas Böhm, Maria S. Novak, Anatolie Gavriluta, Orsolya Dömötör, Jean Bernard Tommasino, Éva A. Enyedy, Sergiu Shova, Samuel Meier, Michael A. Jakupec, Dominique Luneau,* and Vladimir B. Arion*

The reactions of $[Ru(NO)Cl_5]^{2-}$ with glycine (Gly), L-alanine (L-Ala), L-valine (L-Val), L-proline (L-Pro), D-proline (D-Pro), L-serine (L-Ser), L-threonine (L-Thr), and L-tyrosine (L-Tyr) in *n*-butanol or *n*-propanol afforded eight novel complexes, which were characterized by elemental analysis, electrospray ionization mass spectrometry (ESI-MS), ^1H NMR, UV–visible and ATR IR spectroscopy, cyclic voltammetry, and X-ray crystallography.

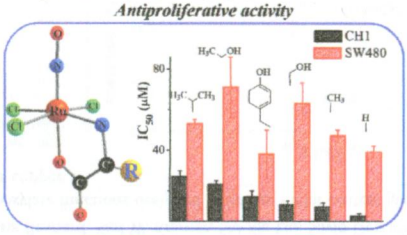

2730 S dx.doi.org/10.1021/ic4031624

Isolobal Analogies in Intermetallics: The Reversed Approximation MO Approach and Applications to $CrGa_4$- and Ir_3Ge_7-Type Phases

Vincent J. Yannello, Brandon J. Kilduff, and Daniel C. Fredrickson*

A straightforward approach is presented to building bonding descriptions of intermetallics: the reversed approximation molecular orbital (raMO) method. Here, we reverse the usual basis set approximation of computations to employ a compound's occupied crystal orbitals as a basis set for determining the eigenfunctions of a simple, chemically transparent model Hamiltonian. We demonstrate the raMO analysis on a familiar molecule, 1,3-butadiene, and then illustrate its use in discovering new bonding phenomena in intermetallic phases.

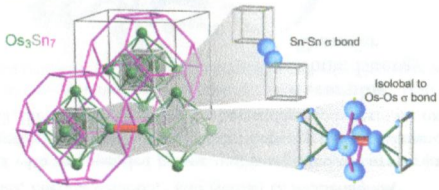

2742 Ⓢ dx.doi.org/10.1021/ic5000843

Three New Alkaline Beryllium Borates $LiBeBO_3$, $Li_6Be_3B_4O_{12}$, and $Li_8Be_5B_6O_{18}$ in the Ternary Phase Diagrams Li_2O–BeO–B_2O_3

Shichao Wang, Ning Ye,* and Guohong Zou

The phase formation in the Li_2O–BeO–B_2O_3 system has been systematical studied by the methods of visual polythermal analysis, spontaneous crystallization, and X-ray diffraction. Three new alkaline beryllium borates, namely, $LiBeBO_3$, $Li_6Be_3B_4O_{12}$, and $Li_8Be_5B_6O_{18}$, were synthesized with molten fluxes based on Li_2O–B_2O_3 solvent in this system. All of the materials are centrosymmetric. The UV–vis diffuse reflectance spectroscopy indicated that the short-wavelength absorption edges of aforementioned materials are all below 200 nm.

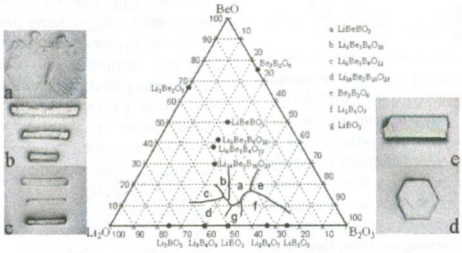

Additions and Corrections

2749 dx.doi.org/10.1021/ic5000099

Correction to Iridium(III) Hydrido N-Heterocyclic Carbene–Phosphine Complexes as Catalysts in Magnetization Transfer Reactions

Marianna Fekete, Oliver W. Bayfield, Simon B. Duckett,* Sam Hart, Ryan E. Mewis, Natalie Pridmore, Peter J. Rayner, and Adrian Whitwood

2750 dx.doi.org/10.1021/ic500270t

Correction to Synthesis, Structure, and H_2/CO_2 Adsorption in a Three-Dimensional 4-Connected Triorganotin Coordination Polymer with a sqc Topology

Vadapalli Chandrasekhar,* Chandrajeet Mohapatra, Rahul Banerjee,* and Arijit Mallick

Ⓢ Supporting Information available via online article